Composites: Part A 205 (2026) 109713

Contents lists available at ScienceDirect

Composites Part A

journal homepage: www.elsevier.com/locate/compositesa

Thermal response and deconsolidation of thermoplastic composite tape during pulsed flashlamp (HUMM3) heating in automated fiber placement (AFP)

Kasahun Niguse Asfew [a,b], Julie Teuwen [b], Daniël Peeters [b,*]

[a] SAM XL - Smart Advanced Manufacturing, Rotterdamseweg 382c, 2629 HG Delft, the Netherlands
[b] Faculty of Aerospace Engineering, Delft University of Technology, Kluyverweg 1, 2629 HS Delft, the Netherlands

ARTICLE INFO

Keywords:
Automated fiber placement (AFP)
Pulsed flashlamp heating (Humm3)
Thermal response
Deconsolidation

ABSTRACT

Laser heating is the most common method in thermoplastic Automated Fiber Placement (AFP) due to its precision and speed, but it poses safety and cost challenges. The HUMM3 pulsed flashlamp offers a promising broadband, programmable, and relatively safer alternative. This study investigates the thermal response and deconsolidation behavior of unidirectional carbon fiber/LM-PAEK (CF/LM-PAEK™) composite tape during HUMM3 heating in AFP. A static setup replicating AFP conditions was used to investigate the thermal response of the composite tape as a function of the programmable parameters: voltage, pulse width and frequency. Deconsolidation of the tape under HUMM3 heating was assessed from micrographs and surface topography, quantified by thickness change, void content, waviness, and roughness. Results showed that voltage is the dominant parameter influencing the thermal response, whereas pulse width and frequency showed no significant effects when total energy input was held constant. The deconsolidation analysis revealed a strong correlation of thickness change, void content, waviness, and surface roughness with local temperature. These changes are believed to be driven by polymer softening, fiber decompaction, internal gas pressure buildup, and local thermal gradients across the tape width. Compared to laser heating, HUMM3 produces less severe deconsolidation, likely due to its broadband UV–VIS–NIR spectrum enabling partial matrix absorption, reducing temperature gradients across the tape width.

1. Introduction

The increasing demand for thermoplastic composite materials in aerospace, automotive, and renewable energy industries has increased the importance of efficient and reliable heating systems in Automated Fiber Placement (AFP). Thermoplastic composites are increasingly adopted for their advantages over thermosets, including recyclability, enhanced toughness, faster processing times, and the potential for in-situ consolidation. In in-situ thermoplastic Automated Fiber Placement, each layer of composite material is consolidated immediately upon deposition, eliminating the need for secondary forming or consolidation processes. However, effective bonding during in-situ consolidation in thermoplastic AFP depends significantly on the processing temperature, compaction pressure, and the time spent above the melt temperature under pressure [1,2]. To meet the heating demands efficiently and reliably, various heating methods have been employed. Among them, laser heating has gained popularity due to its precision and ability to rapidly reach the high temperatures necessary for fast production speeds in thermoplastic AFP. Nevertheless, laser heating comes with safety concerns and requires a laser safety enclosure surrounding the AFP system, which adds to the cost.

As an alternative heating method, a pulsed flashlamp heating system, the HUMM3 from Heraeus Excelitas Noblelight Ltd., has been introduced. This system has the potential to meet the rapid heating requirements for thermoplastic composites while ensuring safer operational conditions [3]. The HUMM3 is a pulsed broadband heater that delivers energy through programmable pulses, with three key parameters: voltage, frequency, and pulse width, referred to as programmable parameters throughout this document. These parameters allow users to tailor the energy input and heat distribution to specific material requirements.

In a Flashlamp Automated Fiber Placement (FLAFP) system, the composite tape and substrate first pass through the heating zone (S1 in Fig. 1), where intense broadband light heats both the substrate and

* Corresponding author.
E-mail address: d.m.j.peeters@tudelft.nl (D. Peeters).

https://doi.org/10.1016/j.compositesa.2026.109713
Received 19 November 2025; Received in revised form 16 February 2026; Accepted 3 March 2026
Available online 11 March 2026

incoming tape to above the matrix melting temperature before they meet at the nip point. Then they move into the consolidation zone (S2 in Fig. 1), where a compaction roller applies pressure starting from the nip point to promote intimate contact and facilitate polymer chain inter-diffusion across the interface, thereby creating a strong interlaminar bond. As the AFP head advances, the material enters the release zone (S3 in Fig. 1), where it cools and solidifies, locking in the bond between layers.

Since the HUMM3 is relatively new in AFP applications, only limited studies have been conducted. Some studies [4–7] have examined the influence of these programmable parameters on the thermal response and bond strength of laminates made from various thermoplastic composites using AFP, for a limited design space of the programmable process parameters. Deden et al. investigated frequency values between 20 and 60 Hz and pulse widths (PW) from 2.5 to 7.5 ms [5], while Legenstein et al. explored frequency ranges of 40 to 80 Hz and pulse widths of 2.2 to 6.2 ms [4]. Expanding the design space of HUMM3′s programmable parameters could provide new insights into how variations in these parameters affect the thermal response of thermoplastic composite tapes.

During the rapid heating in the heating zone, the composite material deconsolidates due to the decompaction of the fiber–matrix network, driven by the release of residual stresses, thermal expansion, and the formation, growth, and coalescence of voids [8]. Several studies have investigated the deconsolidation in composite tapes during the rapid laser heating of CF-PEEK in AFP [8–11]. Unlike lasers, which operate at a single or narrow bandwidth, the HUMM3 heater operates across a broad spectrum (UV–VIS–NIR) [3]. As a result, different absorption characteristics may arise in the composite material, potentially affecting the thermal response or leading to a different temperature distribution in the composite tape. This, in turn, can influence the deconsolidation behaviour of the composite during heating.

This study investigated a broader range of programmable parameters of HUMM3, focusing on how different energy delivery methods (implemented as high-frequency/short-pulse width or low-frequency/long-pulse width combinations under varying voltages) affect the thermal response of CF/LM-PAEK™ unidirectional composite tape. The resulting deconsolidation behaviour under HUMM3 heating, representing the state of the composite tape in the AFP heating zone (S1 in Fig. 1) before entering the consolidation zone (S2 in Fig. 1), was evaluated in terms of thickness change, void content, waviness, and surface roughness. To this end, a static AFP setup was employed, a thermal camera was used to measure thermal response, and deconsolidation characteristics were quantified from cross-sectional micrographs and surface topography of the heated tape.

2. Materials and methods

2.1. Material description

The material used in this study is a unidirectional (UD) thermoplastic composite tape of carbon fiber-reinforced LM-PAEK^{TM} (Toray Cetex® TC1225), supplied by Toray Industries [12]. The tape has a resin weight fraction of approximately 34%, and the pristine tape measured thickness is 160 μm. The neat LM-PAEK^{TM} resin matrix has a glass transition temperature (Tg) of 147 °C, onset of melting temperature (Tm,onset) of approximately 275 °C [13,14], melting temperature (Tm) of 305 °C, and a recommended processing temperature range between 340 °C and 385 °C.

2.2. Experimental setup

A static experimental setup (Fig. 2A), similar to that used by Çelik et al. for a rapid laser heating study [8], was developed to replicate the HUMM3 heating conditions in the heating zone of AFP. This setup was used to study the influence of programmable parameters on the thermal response of the composite tape and to evaluate deconsolidation effects induced by heating. In this setup, the HUMM3 head is mounted at 34.5° relative to the work material (Fig. 2A), mimicking its actual orientation in AFP [6]. The composite tape specimen is positioned in a specimen holder, and a thermal camera was positioned vertically, perpendicular to the specimen, to record temperature evolution during heating.

2.3. Experimental design

Three sets of experiments were designed to investigate the thermal response of CF/LM-PAEK^{TM} composite tape under HUMM3 heating. The first set (Section 2.3.1) employed a full factorial Design of Experiments (DOE) to study the effects and interactions of voltage and frequency–pulse width combination on the thermal response. Tape specimens from this set were also used to examine the deconsolidation behavior of the composite tape due to heating. The second set (Section 2.3.2) employed a subset DOE with shared tape specimens, in which all frequency–pulse width combinations under each voltage were applied to a single tape. This approach avoided specimen-to-specimen variability and enabled assessment of the sole influence of the different energy delivery method on the thermal response. The third set (Section 2.3.3) involved an exploratory study in the lower frequencies and shorter pulse widths to assess the thermal response of the composite tape beyond the DOE-based design space.

2.3.1. Thermal response and deconsolidation behavior of composite tape: full factorial DOE

In this study, a full factorial Design of Experiments (DOE) approach was employed to investigate the thermal response and deconsolidation

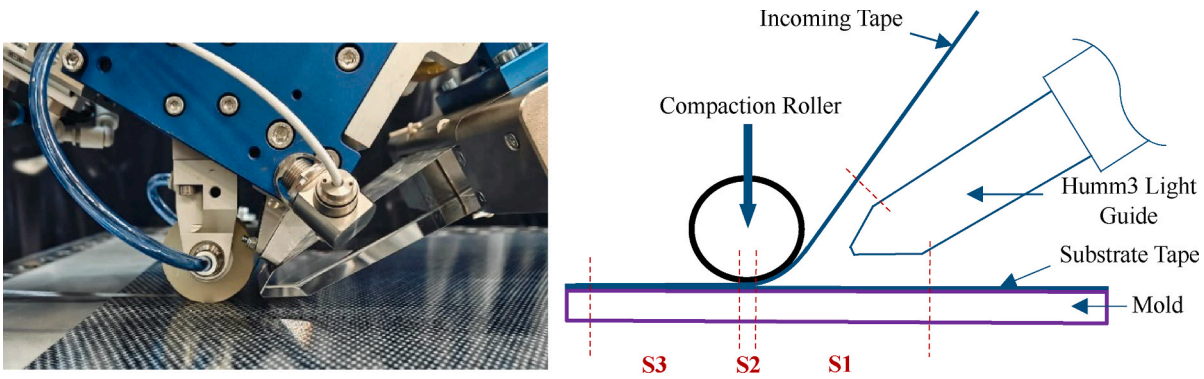

Fig. 1. Flashlamp Automated Fiber Placement (FLAFP) process: (left) AFP head with HUMM3 pulsed broadband heater in operation; (right) schematic representation of heating (S1), consolidation (S2), and release (S3) zones.

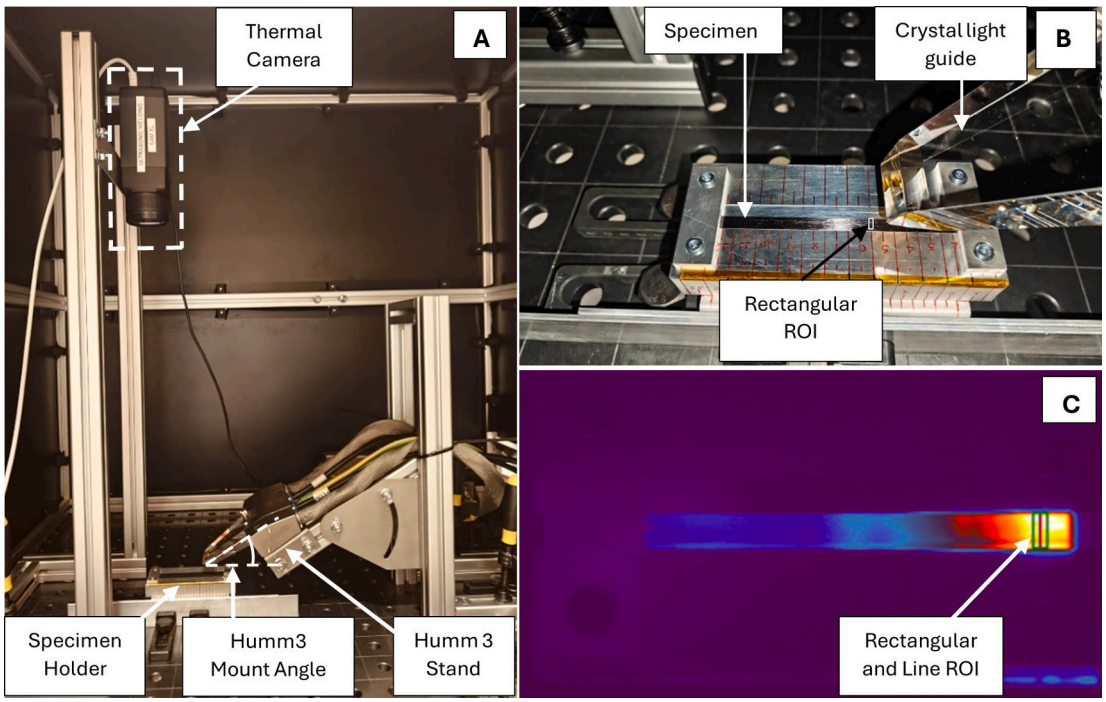

Fig. 2. Static AFP setup with Humm3 (A), Crystal light guide pointing toward the specimen (B), Thermographic image of the specimen during heating, rectangular ROI (green) and line ROI (red) (C).

behavior of composite tape under HUMM3 heating. Two programmable parameters were considered: (1) voltage and (2) frequency–pulse width combination, each evaluated at three levels (Table 1A). The design bounds of the frequency and pulse width levels were considered based on the typical ranges recommended by Heraeus Excelitas Noblelight Ltd. for automated fiber placement, automated tape laying, and filament winding [3].

The voltage levels were selected based on the maximum power capacity of the HUMM3® Discovery version and on levels that could produce composite tape temperatures both below and above the melting point of LM-PAEK™. The frequency and pulse width combinations were selected such that, for each voltage level, the total energy delivered to the specimen remained constant. This enabled us to investigate the influence of different energy delivery methods on the thermal response of the composite tape. All experiments were conducted with a fixed heating duration of 1.2 s. Each unique combination of factor levels was tested in five replicated runs.

2.3.2. *Thermal response evaluation avoiding specimen variability: subset DOE with shared specimens*

This study aimed to evaluate the influence of frequency–pulse width combinations on the thermal response of the composite tape while avoiding variability between tape specimens which could be caused by differences in local fiber volume fraction and variations in thermal contact between the tape and the mold surface, factors known to affect thermal response of a composite material. To address this, all frequency–pulse width combinations under each voltage level were sequentially applied to the same specimen. Each specimen was therefore heated three times (for the three frequency–pulse width combinations), always after cooling down to room temperature. Five specimens were used for each voltage, making a total of ten specimens for the two voltage levels (only the lower, 160 V, and higher, 180 V, levels were considered, as summarized in Table 1B). All runs were conducted with a fixed heating duration of 1.0 s.

Table 1
Test matrix for parametric study: (A) full-factorial DOE and (B) subset DOE using a shared specimen.

Full Factorial DOE (A)		Subset DOE with Shared Specimens (B)	
Voltage (V)	Frequency (Hz) and Pulse width (ms)	Voltage (V)	Frequency (Hz) and Pulse width (ms)
180	60 & 3.0	180	60 & 3.0
170	90 & 2.0		90 & 2.0
160	120 & 1.5	160	120 & 1.5

2.3.3. *Thermal response evaluation in the lower range of frequency–pulse width combinations*

An exploratory study was conducted in the lower range of frequency–pulse width combinations to evaluate the thermal response of the composite tape at lower frequencies and shorter pulse widths, which fall outside the full factorial DOE-based design space described in Section 2.3.1. During these tests, the voltage was fixed at a constant value of 326 V (selected based on the maximum power limit of the HUMM3), while three different frequency (Hz)–pulse width (ms) combinations (20–1.5, 30–1, and 50–0.6), each yielding the same energy level, were considered. All experiments were conducted with a fixed heating duration of 1.0 s. Each run was replicated four times to ensure repeatability of the thermal response measurements.

2.3.4. *Statistical analysis of experimental results*

To evaluate the statistical significance of the programmable parameters on the thermal response of the composite tape, a standard two-way analysis of variance (ANOVA) was employed using a Python script specifically written for this purpose.

2.4. *Thermal response measurement and analysis*

The temperature evolution of the top surface of the tape during heating was captured using a FLIR A655sc thermal camera, which has a resolution of 640 × 480 pixels. Thermal images were recorded at a frame rate of 50 Hz. Post-processing of the thermographic recordings was performed using FLIR Research IR software. To assess the thermal

response of the composite tape during heating, the average temperature within a rectangular region of interest (ROI) measuring 6.35 mm × 1.85 mm, positioned at the center of the heated zone (Fig. 2B and 2C), was extracted from the recordings for all experiments conducted according to the experimental designs described in Sections 2.3.1 to 2.3.3.

In addition, a thermal profile along a line ROI positioned at the center of the heated area across the tape width (Fig. 2C) was used to correlate the thermal response with the resulting deconsolidation characteristics of the tape. This analysis was performed only for the experiments based on the full factorial design described in Section 2.3.1. Both measurements were taken at the end of the heating duration.

2.5. Deconsolidation assessment

The deconsolidation of the composite tape induced by heating was evaluated by analyzing the thickness profile across the tape width, void content, tape waviness, and surface roughness of the heated surface. This deconsolidation represents the state of the composite tape in the FLAFP heating zone prior to entering the consolidation zone. For this evaluation, specimens that resulted in different temperatures, both above and below the polymer's melting point, were selected from the set of experiments conducted according to the full factorial design described in Section 2.3.1.

2.5.1. Waviness and surface roughness measurement and analysis

Surface morphology (waviness and roughness) at the center of the heated region, was measured using surface images collected using Keyence VK-X1000 confocal scanning microscope. Scanning was performed at 20× magnification, and eleven consecutive images were stitched together across the tape width to capture the full waviness and roughness profiles. The measurements were analyzed using Multifile Analyzer software. Following this, the tape specimens were embedded in epoxy and subsequently prepared for cross-sectional micrography, which was used to evaluate thickness change and void content.

Waviness and surface roughness profiles were obtained from the primary profile in accordance with ISO 4287 using Gaussian filters. For the roughness profile, a short-wavelength cutoff of $\lambda s = 80$ μm and a long-wavelength cutoff of $\lambda c = 0.8$ mm were applied. For the waviness profile, the same $\lambda c = 0.8$ mm served as the short-wavelength cutoff, while a long-wavelength cutoff of $\lambda f = 8$ mm was used. To avoid edge effects, data within 100 μm from both edges of the specimen were excluded. Roughness values were extracted from roughness profiles along eleven parallel line profiles, spaced 4 pixels apart and positioned at the center of the heated region (Fig. 3). Quantitative surface roughness, particularly the root mean square roughness (Rq), was used for comparison across different heating levels.

2.5.2. Thickness profile and void content measurement and analysis

The thickness profile and void content of the composite tape were determined from cross-sectional micrography of specimens taken from the center of the heated zone. The specimens were cut 3 mm away from the center of the heated area and embedded in epoxy. During the subsequent grinding and polishing steps, the excess 3 mm was removed. Cross-sectional images were captured using a Keyence VK-X1000 confocal scanning microscope at 20× magnification. To cover the full tape width, eleven consecutive cross-sectional micrographs were acquired and stitched together.

A custom Python code was developed to analyze the stitched micrographs and extract the thickness profile across the tape width. For each specimen, thickness measurements were taken at more than 150 points, enabling the generation of a detailed thickness profile. ImageJ software was used to determine the void content percentage from the cross-sectional images of the specimens. Due to the similarity in grayscale intensity between the matrix and void regions in some areas, automatic thresholding based on grayscale values was not feasible. Therefore, manual segmentation was employed to distinguish the void regions from the matrix and fiber regions. For each micrograph, the void area and tape cross-sectional area were manually identified and quantified, and the void content percentage was calculated as the ratio of the void area to the total cross-sectional area of the tape.

3. Results and discussion

3.1. Thermal response of composite tape

3.1.1. Influence of programmable process parameters: full factorial DOE

The thermal response of the composite tape under different heating conditions was assessed using average temperature at the end of the heating phase. Fig. 4 presents the average surface temperatures at different voltage levels for each frequency–pulse width combination, illustrating how average temperature and its spread (between specimen averages) changes across the design space of the programmable parameters.

Comparing the means of average temperatures for different

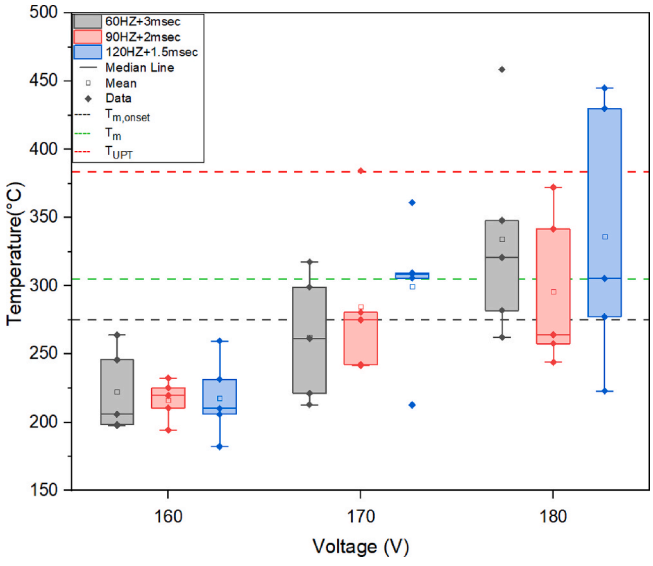

Fig. 4. Average temperature within the rectangular ROI across voltage and frequency–pulse width combinations. Tm, onset: melting onset temperature; Tm: melting temperature; T_{UPT}: upper processing temperature limit.

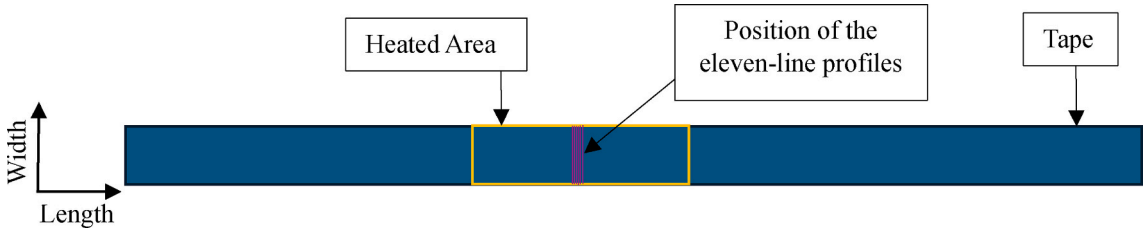

Fig. 3. Illustration of the eleven parallel line profiles positioned across the tape width at the center of the heated region, along which the Rq values were extracted.

frequency and pulse width combinations at a specific voltage level, no clear trend of increase or decrease was established. On the other hand, when comparing the means of average temperatures across different voltage levels (160 → 170 → 180 V) for each frequency–pulse width combination, coded in grey, red, and blue, an increase with voltage is observed.

The two-way ANOVA analysis results on the thermal response of the tape within the design space considered showed that Voltage has a statistically significant effect on the thermal response of the composite tape ($p = 0.000072$). In contrast, the Pulse Width–Frequency combination showed no significant effect ($p = 0.663$), and there was no significant interaction between Voltage and Pulse Width–Frequency ($p = 0.760$).

Contrary to trend reported in the literature [4], where an increase in pulse frequency results in higher tape temperatures than a corresponding increase in pulse width, at the same energy level, the results of this study showed a different outcome. When the total energy input (see Eq. 1) was held constant, changes in frequency and pulse width had an insignificant effect on the thermal response. Instead, voltage emerged as the dominant factor in determining the thermal behavior of the composite material as it changes the supplied energy given by:

$$E_{total} = V^3/K_0^2{*}\tau{*}f \tag{1}$$

where E_{total}: Total energy supplied by the HUMM3 per unit time (J), V: Lamp voltage (V), K_0: Lamp impedance ($\Omega.A^{1/2}$), constant for the given lamp, f: Pulse frequency (Hz), τ: pulse width (s).

Within the design space considered, the thermal response therefore depends primarily on the total amount of energy delivered per unit time, while the distribution of this energy into different frequency-pulse width combinations does not play a significant role.

Furthermore, the spread of average temperature within each group (i.e., between specimens at the same voltage and same frequency–pulse width combination) reflects specimen-to-specimen variability under identical process conditions. This variation suggests that factors other than the programmable parameters influence the thermal response. The most likely contributor could be local fiber volume fraction (FVF) differences across specimens, as also observed by Çelik et al. [8]. The area fraction observed in the cross-sectional micrograph of the pristine tape (Fig. 5) shows noticeable variation: 60.5% in region A and 45.4% in region B. Therefore, specimens with higher FVF in the heated area could absorb more radiative energy, as carbon fibers are highly absorbent across the UV–VIS-NIR range [15], contributing to the variation in thermal response observed between specimens heated under the same conditions. Additionally, uneven contact between the tape and the mold could also contribute, as areas with better contact may conduct more heat to the mold.

The difference in the spread of average temperatures between the frequency–pulse width combinations at a given voltage level (see the box plots under each voltage levels in Fig. 4) is limited. In contrast, the spread increases with increasing voltage for each specific frequency–pulse width combination (see the box plots of the same color across voltage levels in Fig. 4). Higher voltage (i.e., more energy input) amplifies the effects of material and setup inconsistencies. At higher voltage levels, specimens with higher local FVF and poor local contact with the mold might tend to heat up more, widening the spread of average temperatures between specimens.

3.1.2. *Thermal response avoiding specimen variability: subset DOE with shared specimens*

A follow-up investigation was conducted to assess the effect of frequency–pulse width combinations (energy delivery method) on the average temperature of the specimen, while avoiding the influence of specimen-to-specimen variability caused by local differences in FVF and tape-to-mold contact conditions. To achieve this, all frequency–pulse width combinations at each voltage level were applied to the same specimen. This approach enabled us to evaluate the sole effect of the energy delivery method on the thermal response of the tape under a constant total energy input, thereby eliminating the confounding influence of material- and setup-related variations.

Fig. 6 shows the average temperature of each specimen for the three frequency–pulse width combinations (represented in grey, red, and blue) at two voltage levels: 160 V (light yellow background) and 180 V (white background). Since all three frequency–pulse width combinations were applied to the same five specimens at each voltage level (ten specimens in total), only small differences in the average temperatures are observed between the three frequency–pulse width combinations for each specimen. This confirms that the confounding influence of material- and setup-related variations on the evaluation of the effect of the energy delivery method on the thermal response of the composite tape was successfully avoided. The temperature differences observed between specimens in Fig. 6 at a given voltage level are likely attributed to variations in the local fiber volume fraction and tape-to-mold contact conditions, as discussed in Section 3.1.1.

A two-way ANOVA was conducted to evaluate the statistical significance of the effects of voltage, frequency–pulse width combination, and

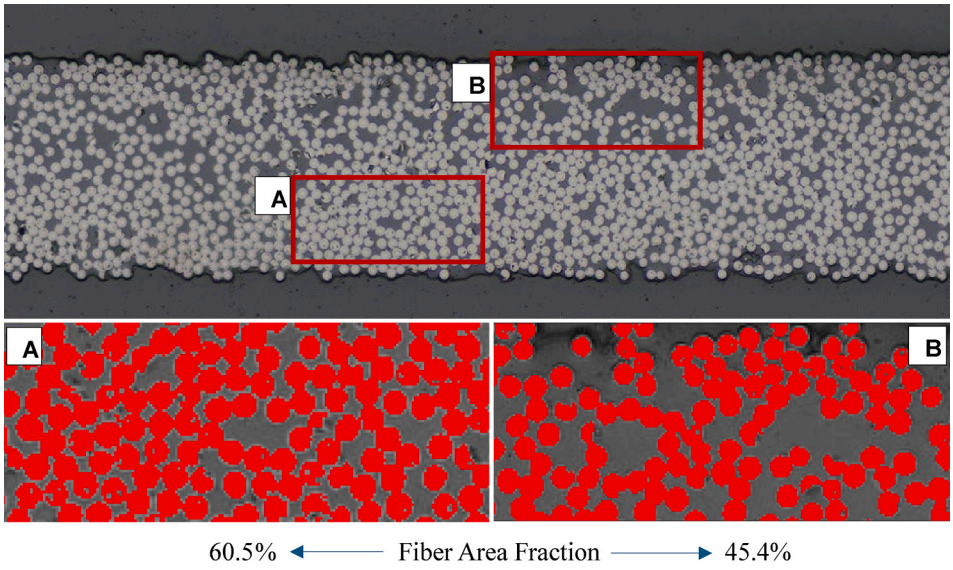

Fig. 5. Local fiber area fraction variation in CF/LM-PAEK^{TM} pristine composite tape.

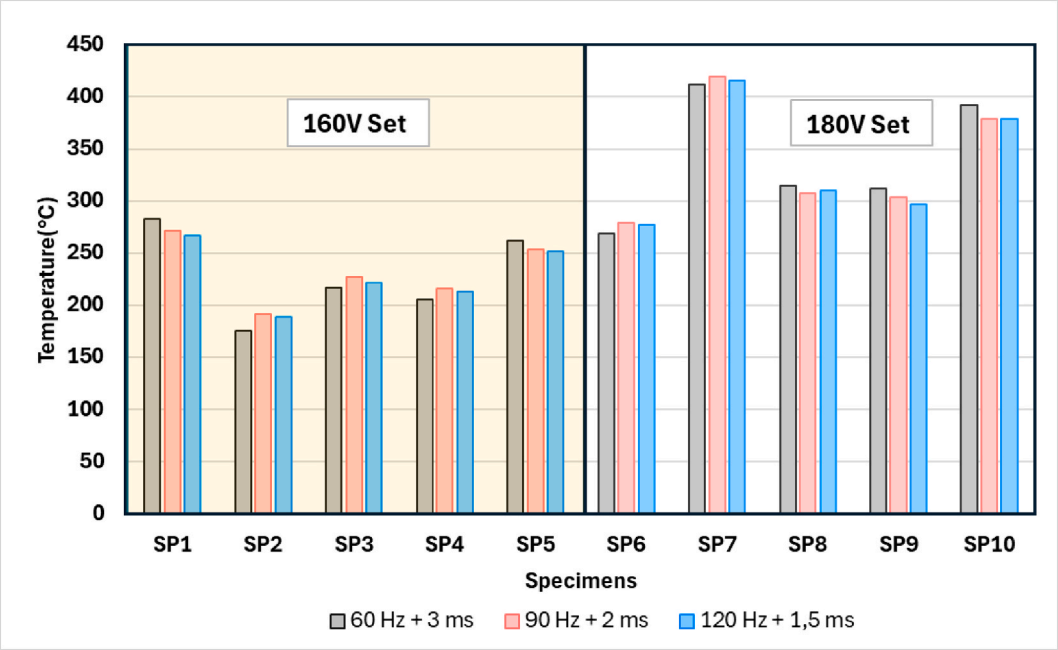

Fig. 6. Average temperature within the rectangular ROI across frequency–pulse width combination at two voltage levels.

their interaction on the thermal response of the composite tape. The results confirmed that voltage had a statistically significant effect on temperature ($p = 0.000003$), while the pulse width–frequency combination showed no significant effect ($p = 0.990$). Furthermore, no significant interaction was found between voltage and pulse width–frequency combination ($p = 0.991$). These results confirm the findings of the full factorial DOE-based experiments: at constant total energy input, varying the energy delivery method does not significantly impact the average surface temperature of the tape.

3.1.3. Thermal response in the lower range of frequency–pulse width combinations

In this section, we assessed the thermal response of the composite tape at the lower range of frequency–pulse width combinations. The aim was to verify whether the earlier observation that varying the energy delivery method does not significantly influence the average surface temperature also holds true in this lower range of frequency–pulse width combinations, which was not included in the full factorial DOE. The average temperature results for each frequency–pulse width combination at a fixed voltage level, where all combinations correspond to the same energy input, are presented in Fig. 7.

A high degree of scatter is observed in the average temperature results, which is likely due to local variations in fiber volume fraction and tape-to-mold contact conditions, as discussed previously. To determine whether the lower frequency–pulse width combinations significantly influence the thermal response of the composite tape, a one-way ANOVA analysis was conducted. Consistent with the findings from the design space explored in the full factorial study, the analysis confirmed that the lower frequency–pulse width combinations considered in this study do not have a statistically significant effect on the average temperature of the composite tape ($p = 0.46$).

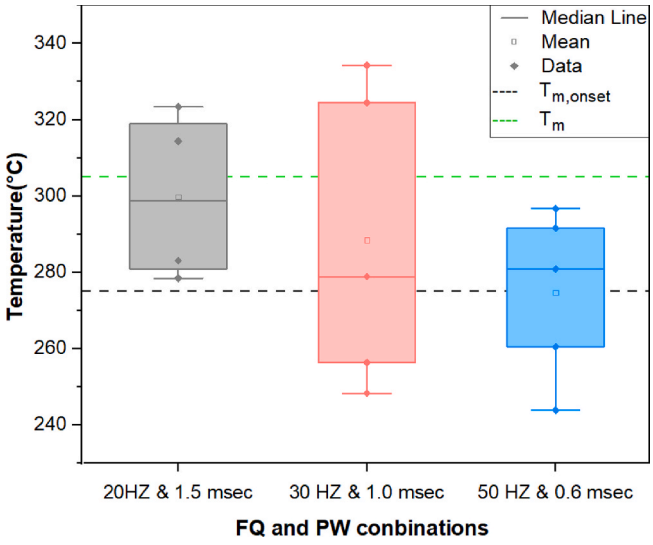

Fig. 7. Average temperature within the rectangular ROI across the lower frequency–pulse width combination at a fixed voltage level.

3.2. Deconsolidation analysis

3.2.1. Thickness change and void content

A. Thickness change

Representative thickness profiles and the corresponding thermal profiles across the tape width of specimens heated to different temperature levels are shown in Fig. 8. The measured average thickness of the pristine tape is 160 μm. In general, the thickness variation across the tape width follows the local temperature distribution. Regions exposed to higher temperatures tend to exhibit increased thickness. Local areas heated above the glass transition temperature (Tg) and up to the onset of melting temperature (Tm,onset), which is approximately 275 °C [13,14], showed only minimal increases in thickness. In contrast, regions heated above 275 °C exhibited significant increases in thickness.

B. Void content percentage

The local void content percentage along each millimeter of the tape width, along with the corresponding thermal profile for selected representative specimens, is presented in Fig. 9. Similar to the trends observed in the thickness profiles, the void percentage also follows the local

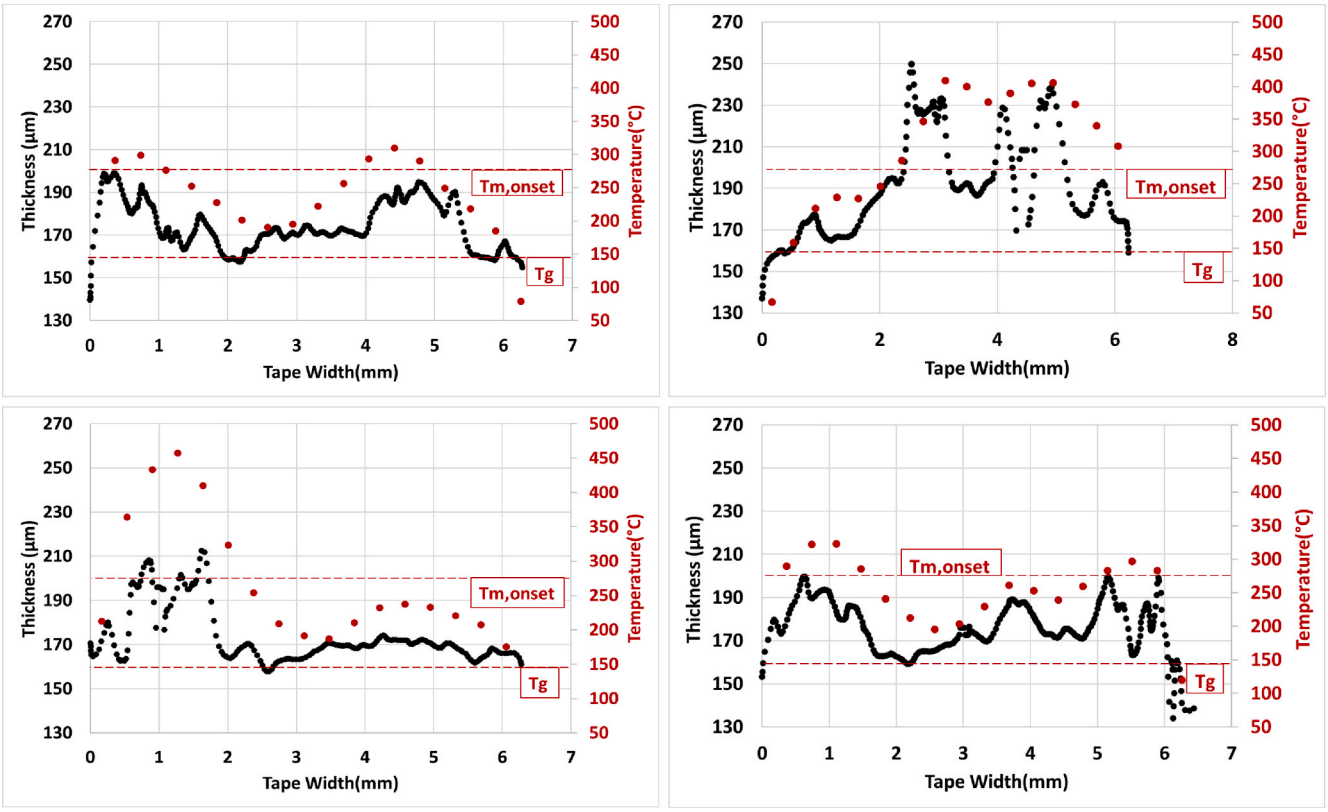

Fig. 8. Temperature profiles (red) and thickness profiles (black) across the tape width of representative specimens.

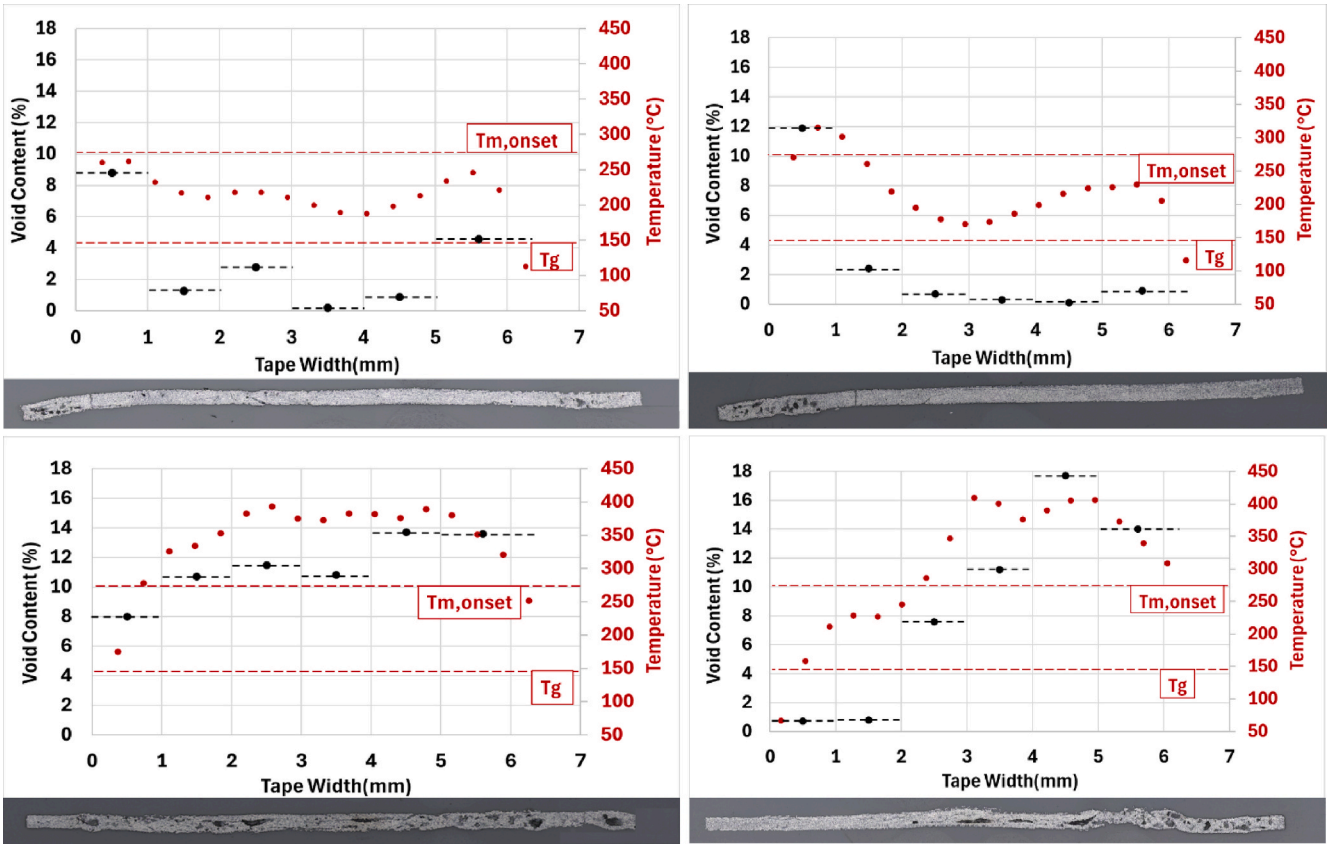

Fig. 9. Temperature profiles (black) and percentage of void content (red) across the tape width of representative specimens.

temperature distribution. Local regions exposed to lower temperatures (below Tm,onset) exhibited relatively low void contents (0.1–6%), whereas areas subjected to higher temperatures (above Tm,onset) showed significantly higher void contents, reaching up to 18%. The cross-sectional images below the plots visually confirm these trends, with specimens heated at excessive temperatures showing pronounced void and deconsolidation characteristics.

The changes observed in the thickness profile and void content may be attributed to the combined effects of rapid heating, matrix behavior, and the absence of external compaction. As reported in previous studies [8], rapid heating can cause vaporization of moisture or residual solvents, originating from prepreg manufacturing or ambient humidity absorption, leading to the buildup of internal gas pressure within the composite. When the matrix softens or melts with increasing temperature, its ability to hold the fibers in place decreases. In the absence of external pressure, the combined effects of internal gas pressure, matrix softening, and residual stresses from manufacturing are believed to promote local fiber bed expansion and decompaction, which in turn may lead to void formation and thickness increase. Because the temperature distribution varies across the tape width, these effects are also likely to be localized.

3.2.2. *Waviness and surface roughness*

The waviness and surface roughness of the composite tape after heating are also analyzed to investigate the surface morphological changes induced by rapid heating with HUMM3. Fig. 10 presents the temperature profile, surface waviness, and surface roughness across the tape width for selected specimens. Both the waviness and surface roughness of the composite tape varied noticeably across its width, showing a strong correlation with local temperature.

In general, regions with higher local temperatures exhibit pronounced peaks in the waviness profile, which consistently coincide with increased surface roughness. A peak in the waviness profile is consistently observed where the temperature locally exceeds Tm,onset and the apex of these peaks aligns with the maximum local temperature. This pattern is most evident in Fig. 10C, particularly in the 0–2 mm region. These waviness peaks are typically accompanied by elevated surface roughness. On the other hand, across all specimens, local areas where the temperature ranges between Tg and Tm,onset exhibit minimal roughness and either less pronounced waviness or a downward-curving (dip) waviness profile.

During heating, local regions where the temperature surpasses Tm, onset may undergo partial matrix melting, leading to local fiber-bed decompaction. As these regions expand and rise due to deconsolidation, the tape surface locally moves closer to the HUMM3 crystal, effectively reducing the distance between the heat source and the tape. This reduced gap can further intensify local heating, thereby accelerating the local decompaction. In contrast, adjacent regions that remain below Tm,onset retain a largely crystalline matrix structure, which preserves sufficient stiffness to restrain fiber movement and resist decompaction. The steep thermal gradient across the tape width thus causes uneven decompaction, inducing local bending moments through the tape thickness. These bending moments likely result in out-of-plane undulations characterized by alternating peaks and dips in the waviness profiles shown in Fig. 10.

Interestingly, in certain regions where the local temperature exceeds Tm,onset but adjacent areas have higher temperatures, the waviness profile forms a dip instead of a peak. This phenomenon is clearly evident in Fig. 10B between 2–3 mm, where the local temperature is high yet lower than in the neighbouring zones (0–1 mm and 3–4 mm). This indicates that in areas where the local temperatures are all above Tm, onset, waviness is also influenced by spatial temperature gradients.

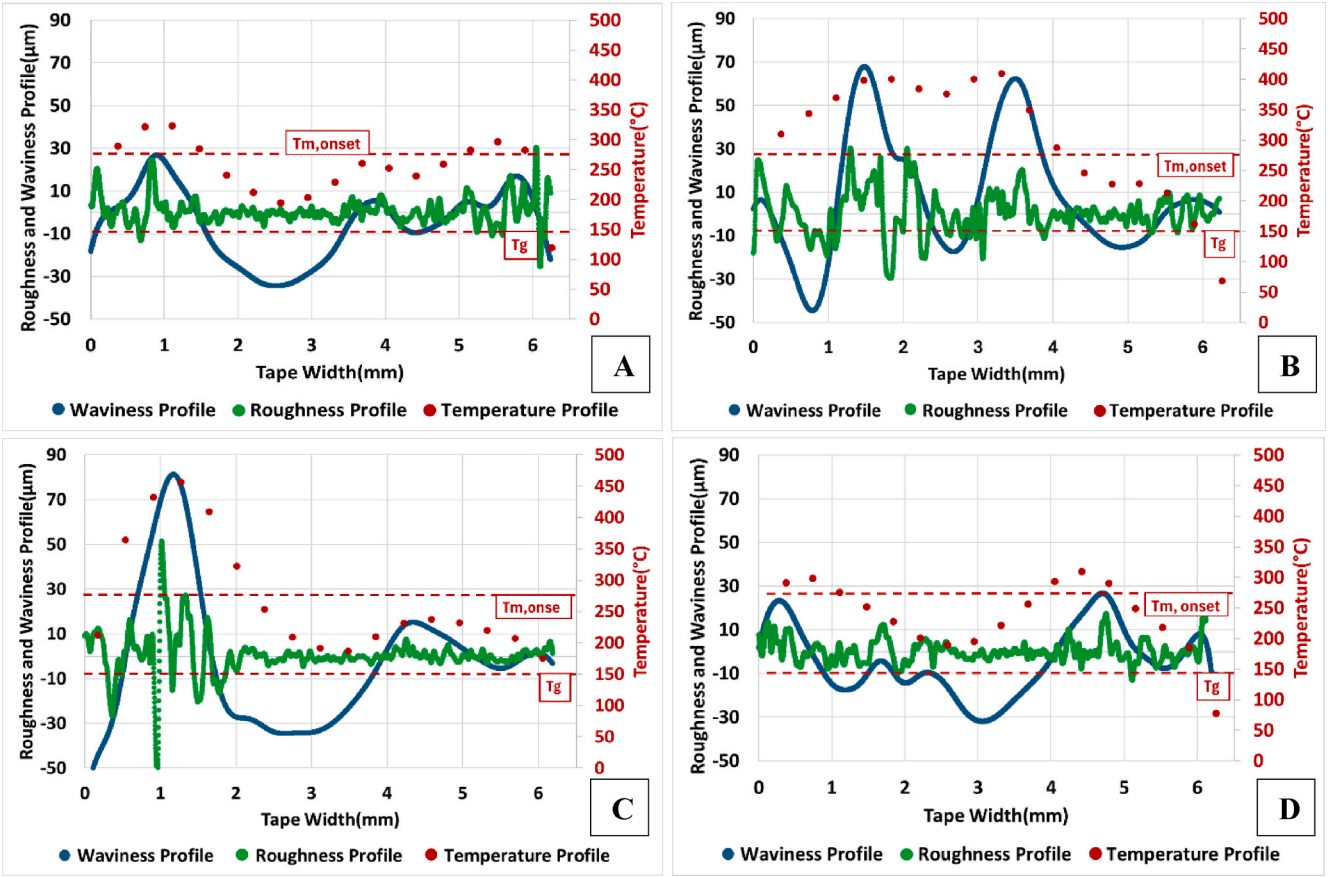

Fig. 10. Temperature (red), surface roughness (green), and waviness (blue) profiles across the width of the composite tape after heating.

The surface roughness is higher in areas where the local temperature exceeds Tm,onset, possibly because local rearrangement of fibers due to fiber bed decompaction, combined with the curvature induced by global waviness, may imprint short-wavelength undulations on the surface, making it rougher. At peak temperature regions, the fiber bed undergoes significant decompaction, and in some cases, individual fibers protrude from the surface, leading to increased surface roughness. In contrast, regions with temperatures below Tm,onset experience limited deconsolidation, as the matrix has not yet begun to melt, leading to relatively lower surface roughness.

To quantitatively assess the surface roughness changes caused by rapid heating with HUMM3, the root-mean-square surface roughness (Rq) was measured for CF/LM-PAEK^{TM} specimens in the pristine condition and heated to an average temperature of 360 °C. The Rq values were first evaluated according to the ISO 4287 defined cut-off lengths, providing a consistent basis for comparing the pristine and HUMM3-heated specimens. To enable a direct comparison with the laser-heated CF/PEEK tape data reported by Çelik et al. [8], the Rq of specimens heated by HUMM3 was also recalculated using the custom cut-off parameters(a short-wavelength (λs) of 96 μm and a long wavelength (λc) of 0.48 mm) adopted in their work.

As presented in Table 2, the pristine CF/LM-PAEK^{TM} tape exhibited a smooth surface with Rq = 1.3 μm (ISO 4287) and 0.9 μm (custom), while the HUMM3-heated specimens showed a substantial increase to 8.1 ± 1.5 μm (ISO 4287) and 5.4 ± 0.5 μm (custom). In comparison, the laser-heated CF/PEEK tape reported by Çelik et al. exhibited Rq = 6.4 ± 0.2 μm (custom), which is slightly higher than that of the HUMM3-heated CF/LM-PAEK^{TM} tape. This may suggest that deconsolidation is more pronounced under laser heating, though material differences may also play a role.

This difference in deconsolidation severity may be attributed to the spectral characteristics of the heating sources and the absorption behavior of the composite tapes. While laser systems typically operate at a single or narrow wavelength, HUMM3 emits a broad spectrum ranging from ultraviolet (UV) to near-infrared (NIR) [3]. Carbon fibers are highly absorbent across both spectral ranges of lasers and HUMM3; however, thermoplastic matrices such as PEEK and LM-PAEK^{TM} are largely transparent within the wavelength range (λ ≈ 940–980 nm) at which NIR diode lasers operate, relying primarily on heat conduction from the fibers [16–19].

In contrast, under UV–VIS–NIR broadband exposure, as in HUMM3, partial matrix absorption becomes possible [20,21]. This absorption may result in a more uniform energy distribution across the tape thickness and width. Supporting this, a dedicated test conducted in this study showed that heating a pure LM-PAEK film using HUMM3 (180 V, 60 Hz, 3 ms pulses for 1 s) resulted in an average temperature of ~ 255 °C, confirming the matrix's direct energy absorption. This might result in more homogeneous heating under HUMM3 and may contribute to the lower deconsolidation rates observed in this study, as it reduces thermal gradients along the tape width, which are among the key drivers of deconsolidation.

Table 2
Mean Rq values for pristine CF/LM-PAEK^{TM} and for heated CF/LM-PAEK and CF/PEEK tapes by HUMM3 and laser, respectively.

Condition	Material	Average Temperature (°C)	Mean Rq (μm): *ISO 4287 cut-off*	Mean Rq (μm): *Çelik et al. custom cut-off*
Pristine tape	CF/LM-PAEK^{TM}		1.3	0.9
HUMM3-heated tape	CF/LM-PAEK^{TM}	360	8.1 ± 1.5	5.4 ± 0.5
Laser-heated tape [Çelik et al.]	CF/PEEK	360		6.4 ± 0.2

Implications for FLAFP. The results of this study provide several insights relevant to the Flashlamp Automated Fiber Placement (FLAFP) process. The thermal response results show that, when the total energy input is kept constant, the energy delivery method (i.e., different frequency–pulse width combinations) does not significantly affect the average temperature of the composite tape. If similar behavior holds under dynamic FLAFP conditions, maintaining a constant voltage level and total energy input per unit time would imply that adjustments or hardware-imposed variations in frequency and pulse width are unlikely to compromise the target nip-point temperature. This observation could simplify control, modeling, and optimization efforts in FLAFP.

In FLAFP, achieving and maintaining an appropriate processing temperature is essential, as the temperature at the nip point governs the development of intimate contact and autohesion between plies, ultimately controlling the degree of consolidation. Although the present study does not directly investigate intimate contact formation under the combined effects of temperature and compaction pressure, the observed specimen-to-specimen variations in thermal response must be carefully considered. These variations arise from local differences in FVF and tape-to-mold contact conditions. During placement, such variations may cause localized underheating or overheating in the heating zone, potentially compromising consolidation in the subsequent consolidation zone. This effect is expected to be particularly critical for the initial layers deposited on a cold metallic mold, where thermal gradients and material interactions are most pronounced.

The deconsolidation characteristics observed in this study reflect the state of the composite tape in the heating zone prior to entering the consolidation zone. In this context, the heating-induced changes in thickness, void content, waviness, and surface roughness quantified in this work, together with their correlation with local temperature across the tape width, define the morphological features of the composite tape that influence subsequent deposition and consolidation processes. A comparison of surface roughness resulting from laser and HUMM3 heating also showed that, at comparable temperatures, HUMM3 heating produces relatively lower surface roughness, suggesting potential advantages of HUMM3 heating in AFP.

Similarly, Khaleghi et al., 2026 showed that the surface morphology of both the substrate and the incoming tape plays a key role in void removal during consolidation [22]. Jamora et al., 2026. demonstrated that tape deformation during AFP deposition is strongly governed by the local temperature distribution in the consolidation zone together with the applied compaction pressure. Thermal gradients lead to non-uniform deformation under the compaction roller, which can promote defect formation [23].

Accordingly, in practical FLAFP operation, it is critical to ensure that both the tape and the substrate remain sufficiently above the polymer's melting temperature upon entering the nip point and are subjected to adequate compaction pressure to eliminate heating-induced deconsolidation effects and promote effective consolidation between plies. For this reason, optimization of parameters such as visible nip-point temperature, compaction pressure, and placement velocity in flashlamp AFP is essential to achieve consistent bonding strength and improved process reliability.

4. Conclusion

This study investigated the thermal response and deconsolidation behavior of unidirectional CF/LM-PAEK^{TM} composite tape during pulsed flashlamp (HUMM3) heating, varying the programmable process parameters (voltage and frequency–pulse width combination), within the operational range relevant to automated fiber placement (AFP). The full factorial DOE study revealed that voltage is the dominant factor influencing the average surface temperature of the tape, as it changes the supplied energy in one pulse. It also showed that frequency–pulse width combinations (the energy delivery method) had no significant impact on thermal response of the composite tape when total energy

input was held constant, and no interaction effects were found. The subset DOE study, conducted to reduce the effects of local differences in fiber volume fraction (FVF) and tape-to-mold contact conditions between specimens, confirmed that frequency– pulse width combinations do not significantly affect the thermal response of the composite tape. An exploratory study conducted to evaluate the thermal response of the composite tape at lower frequency–pulse width combinations that were not included in the full factorial DOE design space also confirmed these findings.

The deconsolidation behavior of UD CF/LM-PAEK™ composite tape subjected to rapid heating using HUMM3 shows a strong correlation with local temperature. Analysis of thickness change and void content reveals that regions exposed to temperatures exceeding Tm,onset undergo significant deconsolidation. At these temperatures, in the absence of external compaction, matrix softening, combined with internal gas pressure generated by the vaporization of volatiles within the tape, might promote fiber bed decompaction, leading to increased thickness and void formation. In contrast, below Tm,onset, the material remains largely stable, exhibiting minimal changes in thickness and void content.

Similarly, the waviness and surface roughness of the composite tape are primarily driven by local temperature. Steep thermal gradients across the tape width and the resulting uneven levels of fiber bed decompaction generate bending moments through the tape thickness, producing waviness characterized by alternating peaks and valleys. At the peaks of the waviness profile, where temperatures are highest, the fiber bed undergoes pronounced decompaction, and in some cases, individual fibers protrude from the surface, increasing surface roughness. Conversely, regions where the temperature remains below Tm,onset exhibit minimal roughness.

In the context of FLAFP, these deconsolidation phenomena occur during the heating stage, where the tape and substrate are rapidly heated before reaching the nip point. The observed deconsolidation characteristics therefore represent the material state after heating in the heating zone but before entering the consolidation zone, where compaction pressure is applied to promote bonding between layers. To eliminate heating-induced deconsolidation effects and ensure effective bonding, both the tape and substrate must remain above the polymer's melting temperature at the nip point and be subjected to sufficient compaction pressure. Compared to laser heating, HUMM3 may cause less pronounced deconsolidation, potentially because its broadband UV–VIS–NIR spectrum enables partial matrix absorption and a more uniform energy distribution. This may reduce thermal gradients across the tape width, a key factor driving waviness and surface roughness.

CRediT authorship contribution statement

Kasahun Niguse Asfew: Writing – review & editing, Writing – original draft, Visualization, Validation, Methodology, Investigation, Formal analysis, Conceptualization. **Julie Teuwen:** Writing – review & editing, Visualization, Validation, Supervision, Methodology, Formal analysis, Conceptualization. **Daniël Peeters:** Writing – review & editing, Visualization, Validation, Supervision, Project administration, Methodology, Funding acquisition, Formal analysis, Conceptualization.

Declaration of competing interest

The authors declare that they have no known competing financial interests or personal relationships that could have appeared to influence the work reported in this paper.

Acknowledgments

The authors acknowledge the funding received for the RDM project "liquid hydrogen composite tank for civil aviation", a subsidy from the R&D Mobily sector arrangement from the ministry of economic affairs and climate, executed by Rijksdienst voor Ondernemend Nederland (RVO).

Data availability

Data will be made available on request.

References

[1] M. J. Donough, Shafaq, N. A. St John, A. W. Philips, and B. Gangadhara Prusty, Process modelling of in-situ consolidated thermoplastic composite by automated fibre placement – a review, Comp. Part A: Appl. Sci. Manuf.
[2] Seneviratne W, Schmitz I, Mcdaniel E. In-Situ consolidation of thermoplastic using automated fiber placement advanced technologies lab for aerospace systems. Thermoplastic composites conference. 2022.
[3] Heraeus Noblelight, Humm3 ®-Journey to industrialisation e-book, (2024).
[4] Legenstein A, Fauster E. Effect of flashlamp heating system parameters on the wedge peel strength of thermoplastic carbon fiber tape in the automated tape placement process. J Manuf Mater Proc 2024;8.
[5] D. Deden, L. Brandt, F. Bruckner, A. Chadwick, and F. Fischer, Optimizing In-Situ Consolidation of Xenon Flashlamp Based Automated Fiber Placement, n.d.
[6] Yadav N, Schledjewski R. Parameter selection for peel strength optimization of thermoplastic CF-PA6 for Humm3™. In: Key engineering materials. Trans Tech Publications Ltd,; 2019. p. 297–302.
[7] L. Brandt, D. Deden, F. J. C. Fischer, F. Bruckner, P. Dreher, D. Williams, M. Engelschall, D. Nieberl, and S. Nowotny, Xenon Flashlamp Based In-Situ Automated Fiber Placement of Thermoplastic Composites, in (Twenty-Second International Conference on Composite Materials (ICCM22), n.d.).
[8] Çelik O, Choudhary A, Peeters D, Teuwen J, Dransfeld C. Deconsolidation of thermoplastic prepreg tapes during rapid laser heating. Compos A Appl Sci Manuf 2021;149.
[9] Amedewovo L, Levy A, de Parscau B, du Plessix J, Aubril A, Arrive LO, et al. A methodology for online characterization of the deconsolidation of fiber-reinforced thermoplastic composite laminates. Compos A Appl Sci Manuf 2023;167.
[10] Slange TK, Warnet LL, Grouve WJB, Akkerman R. Deconsolidation of C/PEEK blanks: on the role of prepreg, blank manufacturing method and conditioning. Compos A Appl Sci Manuf 2018;113:189.
[11] Y. M. Blommert, Deconsolidation of Thermoplastic Prepreg Tapes during the Heating Phase of LAFP, n.d.
[12] Toray Industries, Toray Cetex® TC1225 LMPAEK™ Product Data Sheet, 2023.
[13] S. G. Miller, P. J. Heimann, A. J. Miller, and D. A. Scheiman and L. S. McCorkle, Manufacturing and mechanical testing of TC1225/LM-PAEK and TC1200/PEEK thermoplastic composite panels, NASA/TM-20220015690 (2023).
[14] Raps L, Chadwick AR, Schiel I, Schmidt I. CF/LM-PAEK: Characterisation and sensitivity to critical process parameters for automated fibre placement. Compos Struct 2022;284.
[15] C. Freitag, L. Alter, R. Weber, and T. Graf, Theoretical and experimental determination of the polarization dependent absorptance of laser radiation in carbon fibers and CFRP, 2015.
[16] Stokes-Griffin CM, Compston P. A combined optical-thermal model for near-infrared laser heating of thermoplastic composites in an automated tape placement process. Compos A Appl Sci Manuf 2015;75:104.
[17] Zaami A, Baran I, Bor TC, Akkerman R. Optical characterization of fiber-reinforced thermoplastic tapes for laser-based composite manufacturing. Compos A Appl Sci Manuf 2021;146.
[18] Meister S, Kolbe A, Groves RM. Reflectivity and emissivity analysis of thermoplastic CFRP for optimising Xenon heating and thermographic measurements. Compos A Appl Sci Manuf 2022;158.
[19] Le Louët V, Rousseau B, Le Corre S, Boyard N, Tardif X, Delmas J, et al. Directional spectral reflectivity measurements of a carbon fibre reinforced composite up to 450 °C. Int J Heat Mass Transf 2017;112:882.
[20] Gebauer J, Burkhardt M, Franke V, Lasagni AF. On the ablation behavior of carbon fiber-reinforced plastics during laser surface treatment using pulsed lasers. Materials 2020;13:1.
[21] Jiang W, Chen C, Chen Z, Huang Z, Zhou H. Effect of crystallinity on optical properties of PEEK prepreg tapes for laser-assisted automated fiber placement. Compos Commun 2023;38.
[22] Khaleghi S, Kirchhoff JG, Pandher J, Lacalle J, Tehrani M. Efficient consolidation of thermoplastic composites using AFP-engineered air channels and optimized VBO processing. Compos B Eng 2026;310.
[23] Jamora VC, Sherin CM, Dong S, Bhattacharjee B, Kaipa K, Kravchenko OG. The effect of prepreg laminate thickness on transverse fiber tow deformation during the deposition of AFP composites. Compos A Appl Sci Manuf 2026;201.